IEEE Photonics Journal
An IEEE Photonics Society Publication

Optical Reflection Interference Equalization for Single-Wavelength Bidirectional WDM-PON Transmission System

Volume 13, Number 1, February 2021

Sho Shibita, *Student Member, IEEE*
Daisuke Hisano
Kazuki Maruta
Yu Nakayama
Ken Mishina
Akihiro Maruta, *Member, IEEE*

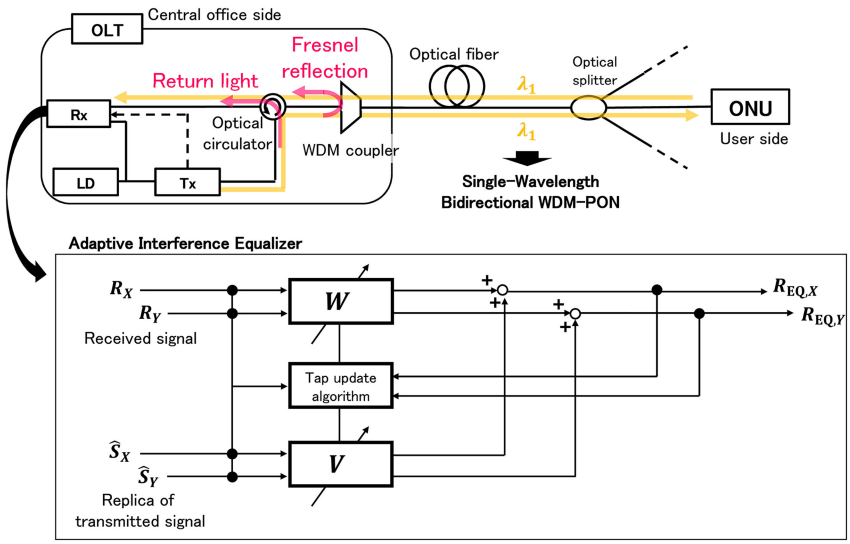

DOI: 10.1109/JPHOT.2020.3045049

Optical Reflection Interference Equalization for Single-Wavelength Bidirectional WDM-PON Transmission System

Sho Shibita,[1] ***Student Member, IEEE***, **Daisuke Hisano**,[1] **Kazuki Maruta**,[2] **Yu Nakayama**,[3] **Ken Mishina**,[1] **and Akihiro Maruta**,[1] ***Member, IEEE***

[1]Graduate School of Engineering, Osaka University, Osaka 565-0871, Japan
[2]Academy for Super Smart Society, Tokyo Institute of Technology, Tokyo 152-8550, Japan
[3]Institute of Engineering, Tokyo University of Agriculture and Technology, Tokyo 184-8588, Japan

DOI:10.1109/JPHOT.2020.3045049

Manuscript received September 7, 2020; revised November 19, 2020; accepted December 11, 2020. Date of publication December 15, 2020; date of current version January 6, 2021. This work was supported by the Telecommunications Advancement Foundation and JSPS KAKENHI under Grants JP19K14982 and JP20H04178. Corresponding author: Sho Shibita (e-mail: shibita@pn.comm.eng.osaka-u.ac.jp).

Abstract: This paper proposes a novel return light cancellation technique using an adaptive interference equalizer in the wavelength division multiplexed passive optical network (WDM–PON) transmission system employing the single-wavelength bidirectional transmission scheme. In this scheme, the same wavelength is assigned to both the uplink and the downlink. In other words, the number of the wavelengths allocated to optical network units can be half compared with a typical PON system. However, this presents us with a problem in that the reflected component of the transmitted signal light interferes with the received signal light. We investigated the performance of the proposed interference canceling equalizer using back-to-back transmission simulation and a dual-polarization-quadrature-phase-shift-keying signal transmission experiment. The results indicated that the proposed adaptive equalizer enabled reception with no error when the OSNR was sufficiently large, even when the power of the interfering light was large (i.e., SIR $\geq$ 2 dB).

Index Terms: Access network system, bidirectional transmission, interference suppression, passive optical network (PON), wavelength division multiplexing (WDM) scheme.

1. Introduction

The spread of passive optical network (PON) systems has been of benefit to many users thanks to broadband services. The next generation of PON systems is expected to accommodate not only services for mass users but also those for business users, for example, future mobile systems such as the sixth generation of the mobile communication system (6 G). However, the conventional time-division multiplexing PON (TDM–PON) system causes delays the order of few milliseconds. It is unsuitable for business users who require low latency. Therefore, to enable PON systems to accommodate multiple services, employing the wavelength division multiplexing (WDM) scheme has been recommended alongside the TDM scheme [1]. In the WDM–PON system, multiple

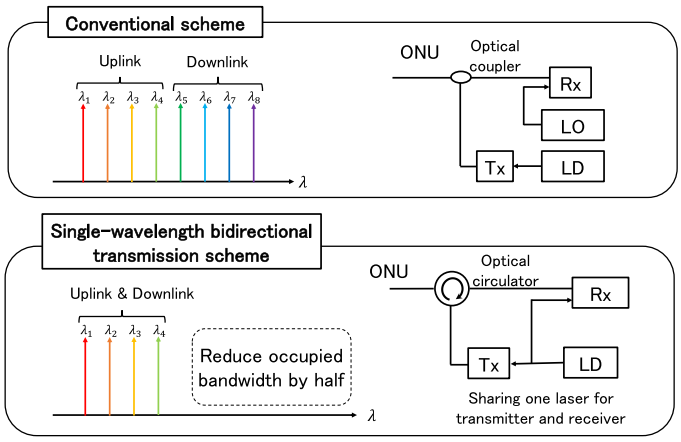

Fig. 1. Comparison of the conventional scheme and the single-wavelength bidirectional transmission scheme.

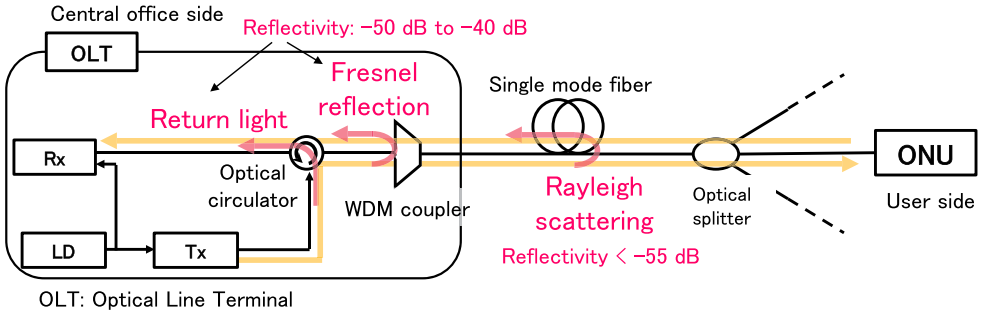

Fig. 2. Reflected lights in the single-wavelength bidirectional transmission scheme.

wavelengths are assigned to each user [2]. In other words, each user is provided with a virtually independent communication channel. This feature eliminates the need for a transmission waiting time in the optical network unit (ONU) to prevent signal collisions, which is necessary for TDM–PON and enables low-latency communication. It is also possible to flexibly set the modulation format according to the bit rate demanded by each user.

However, there is a concern that capital expenditure costs will increase when introducing the WDM–PON system. This condition is because more transceivers operating at different wavelengths will be required as the number of ONUs accommodated in the system increases.

To reduce the introduction cost and improve wavelength utilization efficiency of WDM–PON systems, several studies on a single-wavelength bidirectional transmission scheme have been reported [3]–[6].

In the single-wavelength bidirectional transmission scheme, the same wavelength is assigned to both uplink and downlink. Thus, compared with the typical PON system, the number of wavelengths allocated to ONUs can be half. Fig. 1 shows the configuration of the WDM–PON system, employing the single-wavelength bidirectional transmission scheme and the conventional scheme. In the conventional WDM–PON system, since the wavelengths of the transmitted and received signals are different, the bidirectional transmission is realized by multiplexing and demultiplexing the signals using an optical coupler. In the single-wavelength bidirectional WDM–PON system, since the same wavelength is used for the uplink and downlink, it is necessary to separate the signals using an optical circulator as shown in Fig. 2. The advantage of the single-wavelength bidirectional WDM–PON system is its ability to improve the wavelength use efficiency. Moreover, when the

digital coherent technology is employed in the single-wavelength bidirectional WDM–PON system, the laser light source for the transmitted signal generation can be shared with that for a local oscillator (LO) light at the receiver. Therefore, the number of light sources in the transceiver can be reduced by half.

However, the single-wavelength bidirectional WDM–PON system has a disadvantage that the reflected component of the transmitted signal light interferes with the received signal light. The main components of the reflected light are the return light from the optical devices (e.g., the optical circulator) and the Rayleigh backscattered light generated during fiber propagation. The return light in the optical circulator is generated when a part of the incident light leaks out of ports other than the output ports. The Rayleigh backscattered light is caused by locally refractive index fluctuations in the optical fiber that occur in the manufacturing process. The reflected light interferes with the received signal light and limits the link budget.

This paper proposes an adaptive interference equalizer (AIE) to compensate for the reflected light after the coherent detection to improve the link budget in the single-wavelength bidirectional WDM–PON system. In the proposed AIE, interference compensation occurs on the premise that the reflected light components are known in the receiver as transmission signals. We disclose effectiveness of the proposed scheme through simulative and experimental evaluation.

2. Related Works

2.1 Single-Wavelength Bidirectional Transmission

This section discusses the related works of the proposed scheme. First, we describe a basic study of single-wavelength bidirectional transmission in which the intensity modulation and direct detection (IM–DD) scheme was employed.

The link budget of the bidirectional transmission is limited because the reflected interference light causes signal distortion. The basic characteristics of the limitation of the link budget, when employing the IM–DD scheme with a reflective semiconductor optical amplifier (RSOA), have been reported [4]. RSOA is essentially employed on WDM–PON system based on the IM–DD scheme. The authors [4] investigated the effect of back reflection in a loopback configuration of WDM–PON using the RSOA. In the loopback configuration, the downstream signal was remodulated using RSOA and used for the upstream signal. The reflection tolerance of upstream and downstream signals was evaluated using transmission experiments.

To overcome the limitation of the link budget, a method for suppressing reflective crosstalk in WDM–PON using self-seeded RSOA (SS–RSOA) has been proposed [5]. SS–RSOA is promising in terms of cost; however, the transmitted signal light is degraded by reflective crosstalk in SS–RSOA. In this study, reflective crosstalk is experimentally characterized by its pulse response and the results are used for the pre-equalization of the transmitted signal.

Since the above two proposals are based on the IM–DD scheme, the transmission rate is limited to a few Gbps. Future PONs require high data transmission rates. Our proposal is premised on the use of digital coherent schemes, which can achieve transmission rates over 10 Gbps with a larger link budget.

Next, we introduce a study on single-wavelength bidirectional transmission when the digital coherent scheme is employed. The authors [6] have studied a PON with self-homodyne configurations using RSOA. In this proposed scheme, the pilot tone signal is polarization-multiplexed to the downstream signal at the optical line terminal (OLT). Then, in the ONU, using the polarization beam splitter, the pilot tone signal is separated and input to RSOA for generating the upstream signal. In addition, the signal degradation arising from the reflected light is avoided by applying a frequency shift to the downstream signal through digital signal processing. However, the upstream signal modulation format is limited to binary phase-shift keying (BPSK) or quadrature phase-shift keying (QPSK), hindering the performance of dual-polarization (DP) multiplexing transmission. For the digital coherent-based PON system, a 256-ary quadrature amplitude modulation (QAM) WDM coherent transmission for the next generation of mobile fronthaul has been reported [7]. In [7],

one laser diode (LD) is shared as a transmitter laser and an LO, which enables a cost-effective transceiver. In addition, to mitigate the effects of the reflected light, the light obtained from the LD is frequency-shifted by intensity modulation so that the center frequency of the wavelength of the uplink and downlink is not the same. This proposed scheme requires an LD with a narrower linewidth and an additional intensity modulator for the conventional transceiver. In our proposed scheme in this paper, we employed conventional digital coherent transceivers for both OLT and ONU, without requiring pilot tone signals. Therefore, DP multiplexing transmission was performed without any restrictions on the modulation format of the upstream signal. Moreover, the component of the frequency-shifted scheme was not needed.

2.2 Adaptive Interference Equalizer

In the core optical network, the AIE has been proposed to compensate for inter-channel crosstalk in Nyquist WDM transmission [8], [9]. The proposed scheme suppressed the interference crosstalk from the adjacent frequency channels. The authors [9] employed the successive interference canceller (SIC). The received optical signal-to-noise ratio (OSNR) penalty was improved by iterative demodulation. The popular scheme receives a lower power signal by removing the higher power signal using the SIC. In our proposed scheme, the lower power signal is the interference component, which is the known signal at the receiver end. By removing the known signal using the SIC, the receiver sensitivity of the higher power signal can be improved.

3. Adaptive Interference Equalizer

As shown in Fig. 2, the issue in the single-wavelength bidirectional WDM–PON is that the reflected light, including the return light in the optical circulator, the Fresnel reflection light and the Rayleigh backscattered light, interferes with the received signal light. A theoretical analysis of the reflectivity of the Rayleigh backscattered light has been reported, concluding that it is less than -55 dB [10]. The reflectivity of the Fresnel reflections of the optical devices in the system and the return light of the optical circulator differ for each product, and typically ranges from -50 dB to -40 dB. The circulator is considered to be located much closer to the transmitting light source than other optical devices, and the influence of the return light is expected to be the largest. Therefore, in this section, we propose an AIE to compensate for the return light among these reflected lights.

In the AIE, the interference compensation is performed on the premise that the reflected light components are known in the receiver and generate a replica signal based on this information. In the following section, we first model the received signal vector under the influence of the return light and the Rayleigh backscattered light. Next, we propose a 4×2 multiple-input multiple-output (MIMO) adaptive equalizer to configure the AIE and explain its operational principle.

3.1 Single-Wavelength Bidirectional WDM–PON Model

In this section, we model the received signal vector under the influence of the return light in the optical circulator and the Rayleigh backscattered light.

First, we define the upstream transmission signal vector $\boldsymbol{S}_{\mathbf{u}} \in \mathbb{C}^{2(k+1)}$ from time t to time $t+k$ as follows.

$$\boldsymbol{S}_{\mathbf{u}} = \begin{bmatrix} \boldsymbol{s}_{\mathbf{u}X} \\ \boldsymbol{s}_{\mathbf{u}Y} \end{bmatrix}, \tag{1}$$

$$\boldsymbol{s}_{\mathbf{u}X} = \left[s_{t,X}, s_{t+1,X}, \ldots, s_{t+k,X} \right]^T, \tag{2}$$

$$\boldsymbol{s}_{\mathbf{u}Y} = \left[s_{t,Y}, s_{t+1,Y}, \ldots, s_{t+k,Y} \right]^T, \tag{3}$$

where $\boldsymbol{s}_{\mathbf{u}X}, \boldsymbol{s}_{\mathbf{u}X} \in \mathbb{C}^{(k+1)}$ are the transmission signal vectors, $s_{t,X}$ is the transmission symbol of x polarization, $s_{t,Y}$ is the transmission symbol of y polarization and $[\cdot]^T$ represents transpose. In effect,

the signal continues infinitely. However, for the sake of formulation, we considered only part of finite time width k.

The upstream transmission signal vector passes through the optical fiber channel and is received by the OLT. The received signal vector at OLT $\boldsymbol{R_u} \in \mathbb{C}^{2m(k+1)}$ can be written thus:

$$\boldsymbol{R_u} = \boldsymbol{H_u}\boldsymbol{S_u} + \boldsymbol{N_b} + \boldsymbol{N_i} + \boldsymbol{N}. \tag{4}$$

It is important to note that the size of the column vector is multiplied by m because, in the receiver performs m-fold oversampling for symbol synchronization in the subsequent adaptive equalizer. In this paper, $\boldsymbol{N_b} \in \mathbb{C}^{2m(k+1)}$ is the return light vector in the optical circulator, $\boldsymbol{N_i} \in \mathbb{C}^{2m(k+1)}$ is the accumulated Fresnel reflected light vector generated in the Rayleigh backscattered light and the connection point of the optical device, and $\boldsymbol{N} \in \mathbb{C}^{2m(k+1)}$ is the noise vector generated in the optical amplifier and transceiver. $\boldsymbol{H_u} \in \mathbb{C}^{2m(k+1)\times 2(k+1)}$ is the channel response matrix of the optical fiber uplink and can be expressed as follows:

$$\boldsymbol{H_u} = \begin{bmatrix} \boldsymbol{h_{uXX}} & \boldsymbol{h_{uYX}} \\ \boldsymbol{h_{uXY}} & \boldsymbol{h_{uYY}} \end{bmatrix}, \tag{5}$$

where $\boldsymbol{h_{uXX}}, \boldsymbol{h_{uYY}} \in \mathbb{C}^{m(k+1)\times(k+1)}$ are the channel response matrices for each polarization, $\boldsymbol{h_{uYX}}$, $\boldsymbol{h_{uXY}} \in \mathbb{C}^{m(k+1)\times(k+1)}$ are matrices representing the crosstalk between polarizations.

It is generally difficult to estimate the interference light $\boldsymbol{N_i}$, which includes the Rayleigh backscattered light, because many reflected lights with different reflection points are superimposed. However, the return light $\boldsymbol{N_b}$ in the optical circulator is considered to be the downstream signal light with a distortion. Thus, it can be expressed as follows:

$$\boldsymbol{N_b} = \boldsymbol{H_b}\boldsymbol{S_d}, \tag{6}$$

where $\boldsymbol{S_d} \in \mathbb{C}^{2m(k+1)}$ is the downstream transmission signal vector. $\boldsymbol{H_b} \in \mathbb{C}^{2m(k+1)\times 2(k+1)}$ is a matrix representing the distortion characteristics of the return light. This channel response matrix is also as follows:

$$\boldsymbol{H_b} = \begin{bmatrix} \boldsymbol{h_{bXX}} & \boldsymbol{h_{bYX}} \\ \boldsymbol{h_{bXY}} & \boldsymbol{h_{bYY}} \end{bmatrix}, \tag{7}$$

where $\boldsymbol{h_{bXX}}, \boldsymbol{h_{bYY}} \in \mathbb{C}^{m(k+1)\times(k+1)}$ are the channel response matrices for each polarization, and $\boldsymbol{h_{bYX}}, \boldsymbol{h_{bXY}} \in \mathbb{C}^{m(k+1)\times(k+1)}$ is a matrix representing the crosstalk between polarizations. Since the OLT transmits the downlink transmission signal $\boldsymbol{S_d}$, its symbol sequence is naturally known.

3.2 4 × 2 MIMO AIE

In this section, we propose a configuration of the AIE using a 4×2 MIMO adaptive equalizer and explain its operational principle. Fig. 3 shows the proposed adaptive equalizer. The received signal vector $\boldsymbol{R_u}$ and the replica signal $\hat{\boldsymbol{S}}_\mathbf{d}$ of the downlink transmission signal are input to the adaptive equalizer. Common adaptive equalizers in the digital coherent system adopt a 2×2 MIMO configuration to perform polarization demultiplexing. However, the proposed AIE has a 4×2 MIMO configuration because the replica signal is prepared and input in x and y polarizations alongside the received signal. The replica signal is generated by shaping the waveform of the downlink signal transmitted from the OLT. In other words, the known downlink transmission signal $\boldsymbol{S_d}$ is m-fold up-sampled and passed through the Nyquist filter used in the transmitter. When the output of the equalizer is $\boldsymbol{R_{EQ}}$, the relationship between the input and the output can be written as follows:

$$\boldsymbol{R_{EQ}} = \boldsymbol{W}\begin{bmatrix} \boldsymbol{R_X} \\ \boldsymbol{R_Y} \end{bmatrix} + \boldsymbol{V}\begin{bmatrix} \hat{\boldsymbol{S}}_{d,X} \\ \hat{\boldsymbol{S}}_{d,Y} \end{bmatrix}, \tag{8}$$

where $\boldsymbol{W}, \boldsymbol{V} \in \mathbb{C}^{2(k+1-w)\times 2m(k+1)}$ are the tap matrices of the equalizer and w is the tap number of the equalizer.

The replica signal $\hat{\boldsymbol{S}}_d$ is shaped an ideal rectangular waveform. This shape may not be same as that of the original signal $\boldsymbol{S}_d$. However, the adaptive filter can adjust the pulse shape automatically

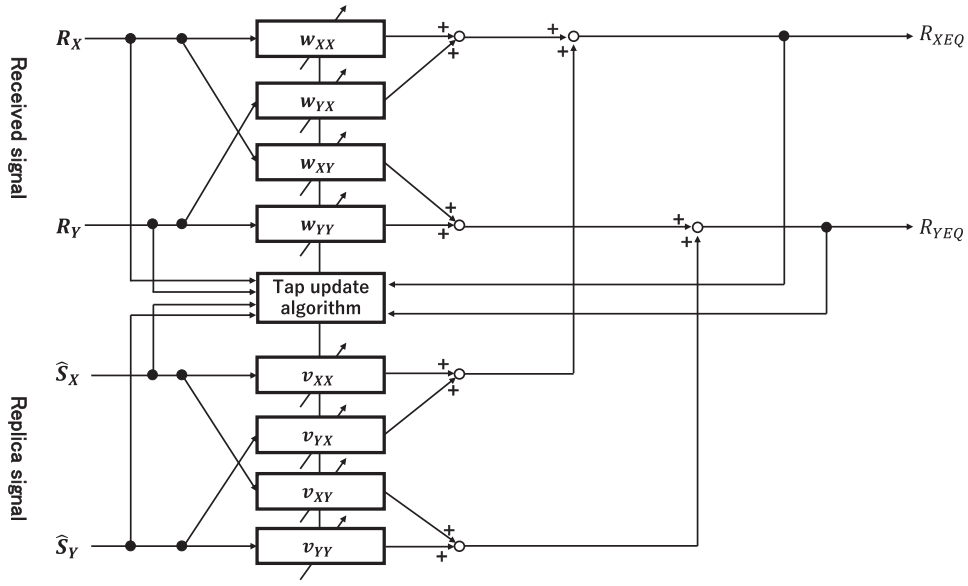

Fig. 3. Proposed 4 × 2 MIMO adaptive equalizer.

with the tap update. In this formulation, the output signal is shorter than the input signal by the number of taps. In practice, however, zero padding will be added to both ends of the signal, so no information about the signal will be missing.

$\boldsymbol{W}$, $\boldsymbol{V}$ are expressed as follows:

$$\boldsymbol{W} = \begin{bmatrix} w_{XX} & w_{YX} \\ w_{XY} & w_{YY} \end{bmatrix}, \ \boldsymbol{V} = \begin{bmatrix} v_{XX} & v_{YX} \\ v_{XY} & v_{YY} \end{bmatrix}. \tag{9}$$

The insertion of (4) and (6) into (8) yields the following result:

$$\boldsymbol{R_{EQ}} = \boldsymbol{W}(\boldsymbol{H_u S_u} + \boldsymbol{H_b S_d} + \tilde{\boldsymbol{N}}) + \boldsymbol{V}\hat{\boldsymbol{S}}_\mathbf{d}, \tag{10}$$

where $\tilde{\boldsymbol{N}} = \boldsymbol{N_i} + \boldsymbol{N}$. In the equalizer, the tap coefficients are adjusted to satisfy $\boldsymbol{W H_u} = \boldsymbol{I W H_b} + \boldsymbol{V} = \boldsymbol{O}$, and the final output $\tilde{\boldsymbol{R}}_{\mathbf{EQ}}$ is as follows.

$$\tilde{\boldsymbol{R}}_{\mathbf{EQ}} = \boldsymbol{S_u} + \boldsymbol{Z}, \tag{11}$$

where $\boldsymbol{Z}$ is a term that summarizes the reflected light caused by Rayleigh scattering, and the noise given to the upstream signal and the return light. As can be seen from the discussion above, the proposed method is designed to suppress the reflected light from isolated reflection points and cannot deal with reflections where the reflection points are uniformly distributed over the entire fiber, such as Rayleigh scattering. The method to avoid the Rayleigh backscattering as much as possible has been proposed [11]. Both proposed method can be combined.

In our proposed scheme, even when the AIE has the timing offset between the interference signal and the replica signal, the interference suppression can be achieved. This is because the tap weights of the AIE are automatically adjusted. When the timing offset is larger than the tap length, a coarse alignment will be required to keep it within the tap length. Since the amount of timing offset depends on the distance to the reflection point, the coarse alignment can be achieved by roughly estimating the distance in the system design process and then using that value to delay the replica signal.

Moreover, the proposed 4 × 2 MIMO AIE is designed to suppress the effect of the interference light from a single reflection point, but in a real system, there may be multiple reflection points that affect the received signal. In such a case, by extending the above discussion, it is shown that the

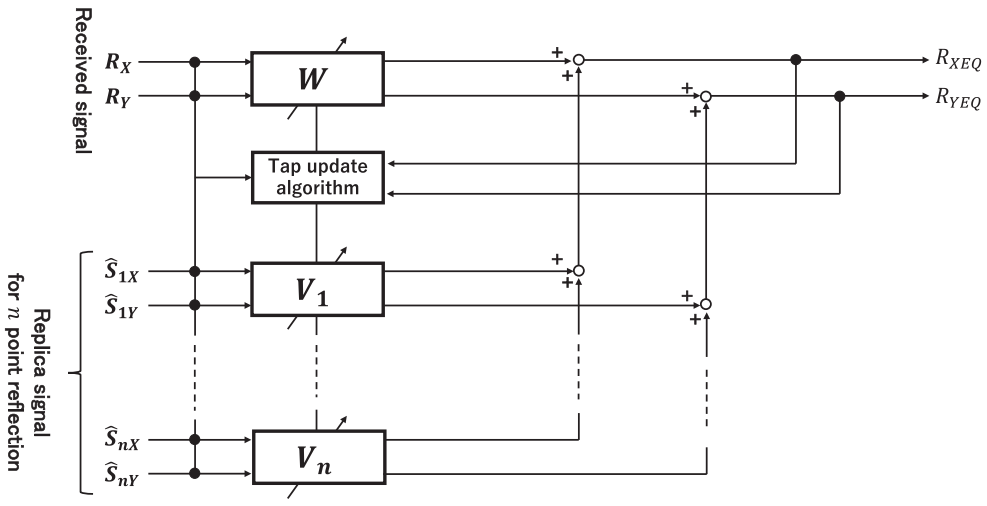

Fig. 4. Proposed adaptive equalizer corresponding with n point reflection.

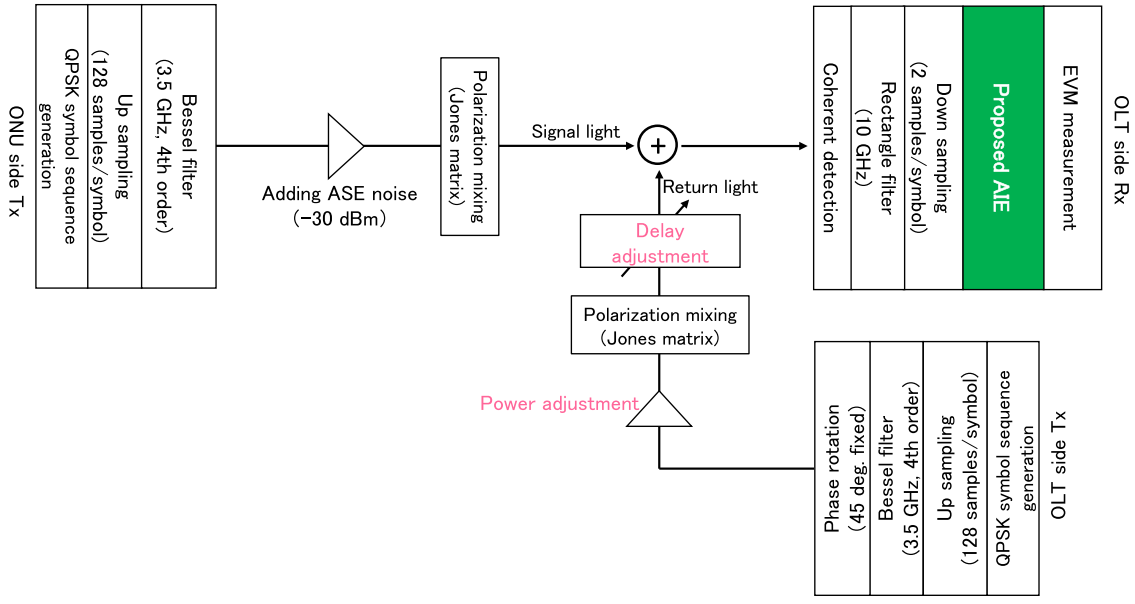

Fig. 5. Simulation setup.

AIE for n point reflection can be implemented in a $2(1+n) \times 2$ MIMO configuration as shown in Fig. 4.

4. Numerical Simulation

4.1 Setup

This section presents the results of the performance evaluation of the AIE using a back-to-back transmission simulation. Fig. 5 displays the simulation setup, and Table 1 shows the simulation parameters. The transmission signals from the OLT and ONU were DP–QPSK signals with symbol rates of 10 Gbaud and were excessively bandwidth-limited to 3.5 GHz by 4th order Bessel filter

TABLE 1
Simulation Parameters

Parameter	Value
Modulation format	DP–QPSK
Symbol rate	10 Gbaud
Algorithm for adaptive equalization	Least mean square (LMS)
Tap number w of adaptive equalizer	15 taps
Oversampling rate m in the receiver	2 samples/symbol
Step size of adaptive equalizer	0.0016
The number of training symbols	5000 symbols

to match the bandwidth of the arbitrary waveform generator (AWG) used in the experiments described in Section 5. Then, the signals were polarization-mixed with a Jones matrix because there exists crosstalk between the two polarization channels, even in back-to-back transmission. In the functional blocks simulating the receiver of the OLT, the AIE conducted polarization demultiplexing, symbol synchronization, and interference equalization.

For the return light generated by the optical circulator, some kind of distortion can be assumed to have been added to the downstream signal light transmitted from the OLT, as described in Section 3. In this simulation, we simply assumed that the distortions caused by reflections in the optical circulator were attenuation and phase rotation. The QPSK signal generated in the OLT was attenuated and phase-shifted to simulate the return light. We set the value of phase rotation to 45 degrees because the distance between the received signal point on the constellation map and the threshold line of the symbol decision is the closest in this case. In other words, we simulated the worst reception conditions.

4.2 Signal-to-Interference Power Ratio Characteristics

The simulation evaluated the signal-to-interference ratio (SIR) characteristics where the symbol timing between the signal and the interference perfectly matched. (Hereafter, we will refer to this as "interference timing is matched.") In this situation, the error vector magnitude (EVM) was measured by varying the SIR.

The SIR was adjusted by adding the interference signal where the average power ranged from -20 to -2 dBm in relation to the transmitted signal from the ONU where the average power was fixed at 0 dBm. Fig. 6 shows the result of the measured EVM. In the absence of interference signals, the EVM was 9.2%. The EVM was significantly degraded without the AIE when SIR decreased. With the proposed AIE, the EVM can be kept to almost the same level as the value in the case of no interference signal. The simulation results confirmed that the degradation of the EVM arising from the return light was almost completely suppressed by the proposed AIE.

4.3 Interference Timing Offset Characteristics

The SIR was fixed at 3 dB, and the EVMs were evaluated when the interference timing offset was changed by adjusting the delay of the interference signal. The time width of the symbol was 100 ps because the symbol rate was set to 10 Gbaud in this simulation. Therefore, varying the amount of delay of the interference signal with a width of 100 ps was sufficient for evaluating the interference timing characteristics. This simulation varied the amount of delay from 0 ps to 100 ps.

The measured EVM are shown in Fig. 7. A delay of 0 ps corresponds to the state in which the interference timing is perfectly matched. There was no effect on the equalization performance due to the misalignment of the interference timing.The EVM without AIE fluctuates as the timing offset changes, but this only occurs when the signals are excessively bandwidth-limited.

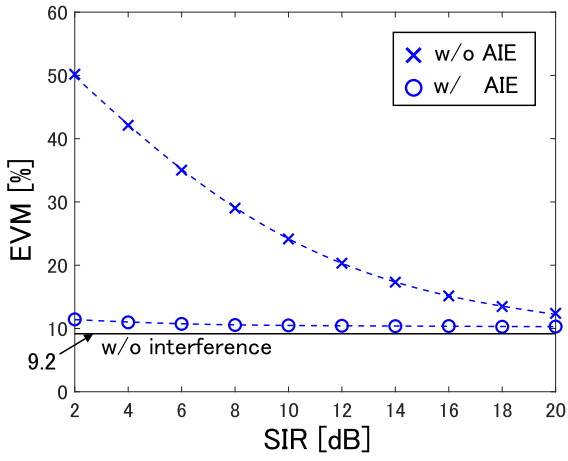

Fig. 6. EVM vs. SIR w/ and w/o the proposed scheme.

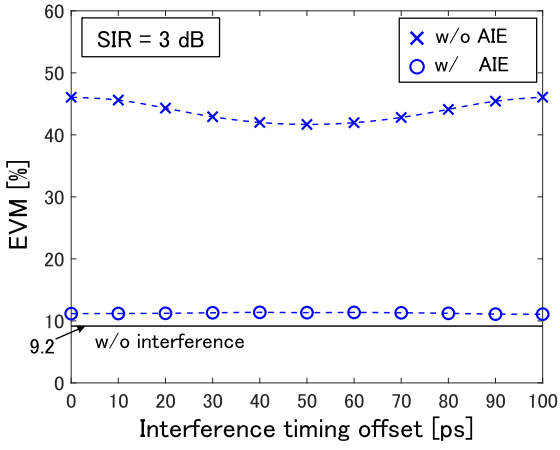

Fig. 7. Influence of interference timing offset.

4.4 Performance of AIE for Two-Point Reflection

The SIR characteristics were evaluated for the case with two reflection points. We increased the number of blocks generating the return light to two and changed the configuration of the AIE to 6×2 MIMO for the simulation. The other parameters are the same as in Table 1. As in Section 4.2, the SIR of each return light was varied from 2 dB to 20 dB by fixing the signal light power at 0 dBm and adjusting the return light power. The results of the EVM measurements are shown in Figs. 8 and 9 as contour lines. They show that the performance of AIE for two-point reflection is constant regardless of the magnitude of the two return light powers. Even in the case of more than three reflection points, it is possible to suppress the interference component by increasing the number of AIE inputs as shown in Fig. 4.

5. Experiments

In this section, the principle of the experiment was tested to confirm the effectiveness of the proposed method. The three evaluation items are as follows:

1) Bit error rate (BER) and EVM when SIR varies.
2) BER when SIR is fixed and OSNR varies.

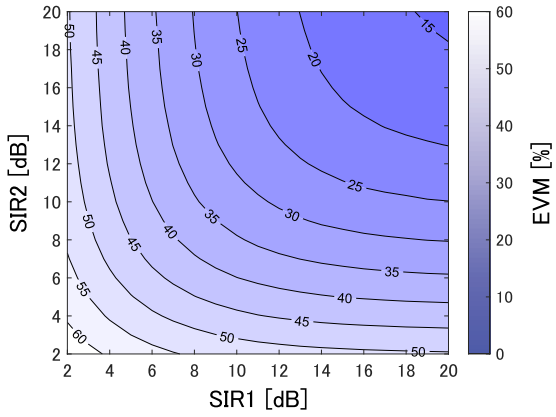

Fig. 8. SIR characteristics for two-point reflection (w/o AIE).

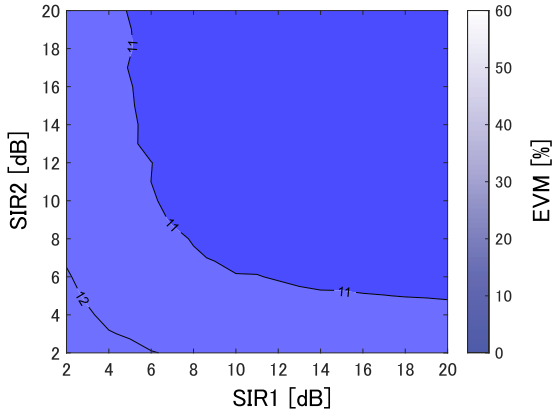

Fig. 9. SIR characteristics for two-point reflection (w/AIE).

3) Impact of interference timing offset.

5.1 Experimental Setup

Fig. 10 exhibits the experimental setup. Table 2 shows the experimental parameters. The LD with a linewidth of 100 kHz initiated the continuous wave (CW) light into the 3 dB optical splitter. The split CW light was input into an in-phase/quadrature (IQ) modulator to generate a signal and an interference light. The other split CW light was transmitted to a coherent receiver to be used as the LO light. Strictly speaking, the interference light and LO light were used the same as the LD, as described in Section 1. In other words, the LD of the signal light and interference light is different. However, this experiment drew on self-homodyne detection due to the limitation of our experimental equipment.

For the signal generation, we prepared two pseudo-random bit sequences (PRBSs) of $2^{15} - 1$. We input the PRBSs into the AWG 7122 C operated by Tektronix, Inc. The 2-channel analog electric signals were input into the IQ modulator, and then a single-polarization (SP) QPSK optical signal was generated. The SP–QPSK signal was transmitted to a polarization multiplexing emulator (PME) with a 20 m delay line. The PME converted the SP–QPDK signal into the DP–QPSK signal. In this experiment, we generated the signal light and the reflected light from the DP–QPSK signal originating from the PME. The DP–QPSK signal was split by the 3 dB optical splitter. The split DP–QPSK signal that had propagated through a 20 km single-mode fiber (SMF), was used as the

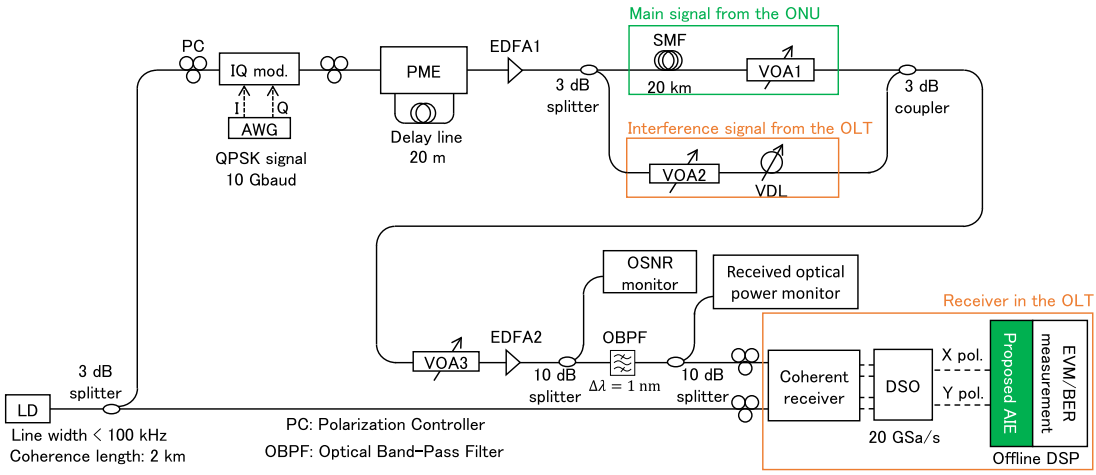

Fig. 10. Experimental setup.

TABLE 2
Experimental Parameters

Parameter	Value
Modulation format	DP–QPSK
Symbol rate	10 Gbaud
Transmission length	20 km
Coherence length of LD	2 km
Sampling rate of digital storage oscilloscope (DSO)	20 GSa/s
Algorithm for adaptive equalization	Least mean square (LMS)
Tap number w of adaptive equalizer	15 taps
Oversampling rate m in the DSO	2 samples/symbol
Step size of adaptive equalizer	0.0016
The number of training symbols	5000 symbols

main signal light. The other split DP–QPSK signal was used as the interference light. The main signal and the interference light were coupled by the 3 dB optical coupler. The SIR was adjusted by the two variable optical attenuators (VOAs) between the optical splitter and the optical coupler. The timing offset of the interference was adjusted by the variable delay line (VDL) located in the optical transmission line of the interference light.

The LD has a linewidth of 100 kHz and a coherence length of 2 km. Therefore, the signal light and the LO light have a path difference of more than 10-fold the coherence length owing to a 20 km SMF. They can be considered to have been generated from different light sources with the same center frequency. Since the LO light and the interference light have a path shorter than the coherence length, they can be considered to have been generated from the same light source. Therefore, it is possible to emulate the situation of the single-wavelength bidirectional transmission scheme using this experimental system except for the carrier frequency offset between the signal light and the LO light.

After coupling the signal light with the interference light, VOA3 and erbium-doped fiber amplifier (EDFA) 2 adjusted the OSNR. It is important to note that the terms of the signal power of the OSNR include the power of the interference light. DSO-X 95004Q, operated by Keysight Technologies, performed 20-GSa/s. In other words, the oversampling rate was two samples/symbol. The tap

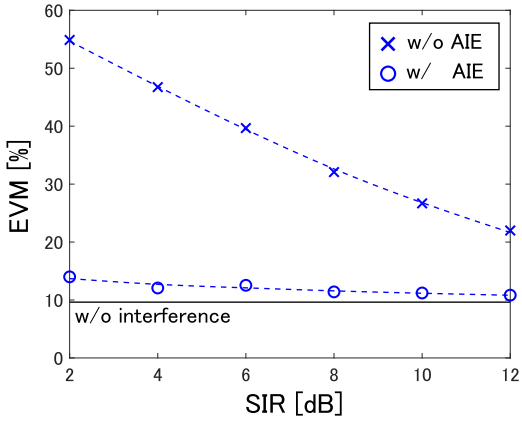

Fig. 11. EVM vs. SIR w/ and w/o the AIE.

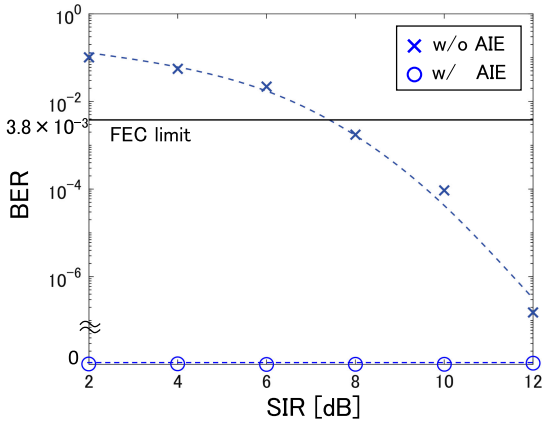

Fig. 12. BER vs. SIR w/ and w/o the AIE.

updating algorithm of the proposed AIE was employed as the LMS algorithm. After the proposed AIE, the BER and EVM were measured. The digital signal processing for the demodulation including the equalization was performed in the offline state.

5.2 SIR and OSNR Characteristics

We evaluated the EVM and BER by varying the SIR. VOA1 and VOA2 were used to vary the SIR by fixing the average power of the main signal at 0 dBm and varying the average power of the interference signal from -12 to -2 dBm. These signals were combined with a 3 dB coupler, amplified by EDFA2, and received by a coherent receiver. The OSNR was measured after EDFA2, and its signal component is the sum of the signal light and the interference light. The measured value of OSNR was 22 dB when SIR $=$ 2 dB.

Figs. 11 and 12 show the measurement results of EVM and BER curves. The EVM without the return light was 9.6 %, and no bit errors were observed. No bit errors were also observed when using the AIE, and Fig. 12 shows only the case without AIE. The results suggest that the proposed equalizer can improve the BER below the forward error correction (FEC) limit even when the SIR is small as observed in the simulation results.

Subsequently, we evaluated the BER for SIRs of 4 and 6 dB by varying the OSNR using VOA3 and EDFA2. The results are shown in Figs. 13 and 14. The BER was greatly improved with the AIE

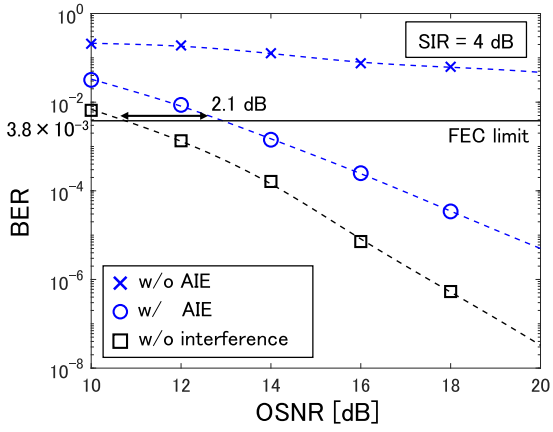

Fig. 13. BER vs. OSNR w/ and w/o the AIE (SIR = 4 dB).

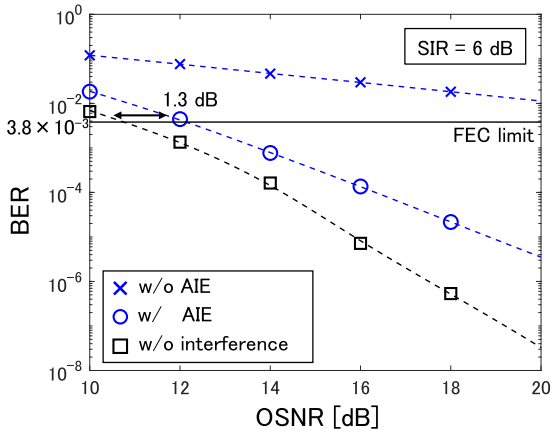

Fig. 14. BER vs. OSNR w/ and w/o the AIE (SIR = 6 dB).

and the quality of reception was almost the same as in the absence of interfering light. However, there was a slight penalty. The reason for this is that the interfering light was generated by branching the signal light, and the interfering light also contained noise. Moreover, we set the received power to the constant value and adjusted the OSNR of the signal light including the interference light in this experiment. In this situation, when the SIR decreases, the signal light power also decreases, however the noise power does not change. Therefore, the OSNR of the signal light including the interference light degraded when the SIR decreased. This is reflected in the degradation of the OSNR penalty.

5.3 Interference Timing Offset Characteristics

We also tried to determine whether the interference timing offset between the signal light and reflected light had any impact on the performance of the proposed equalizer. We varied the amount of delay of the interfering light, which was regarded as the reflected light, from 0 to 100 ps by VDL with the SIR being fixed at 3 dB. We also investigated the changes in EVM and BER with and without the AIE. The receiving power was adjusted to 0 dBm by EDFA2. The results are shown in Figs. 15 and 16. We confirmed that the interference timing offset did not affect the performance of the AIE as well as the simulation results.

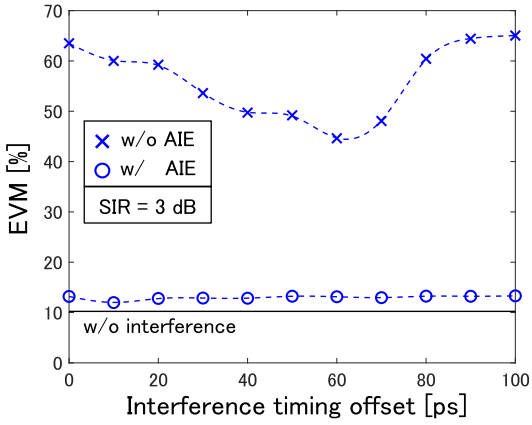

Fig. 15. EVM vs. interference timing offset (SIR = 3 dB).

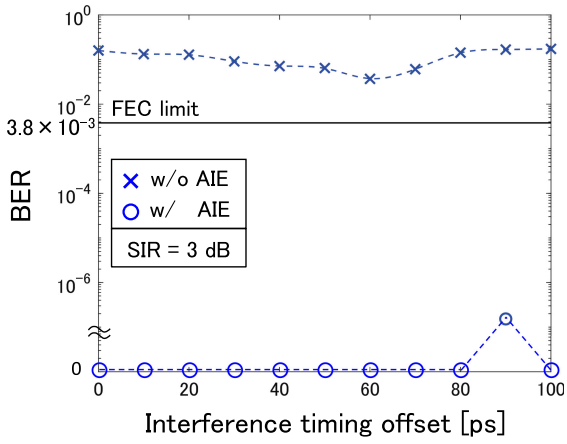

Fig. 16. BER vs. interference timing offset (SIR = 3 dB).

6. Conclusion

In this paper, we proposed an AIE to compensate for the return light generated by an optical circulator that limits the link budget in the single-wavelength bidirectional WDM–PON transmission scheme. We investigated the performance of the proposed equalizer in a DP–QPSK signal transmission experiment in a self-homodyne configuration. The results indicated that the proposed adaptive equalizer enabled reception with no error when the OSNR was sufficiently large, even when the power of the interfering light was large (i.e., SIR $\geq$ 2 dB).

Moreover, the proposed AIE can be realized with only a few modifications to the adaptive equalizer used in the conventional digital coherent scheme. Therefore, this proposal can not only be applied to WDM–PON but also any optical communication system that relies on digital coherent transmission systems.

References

[1] K. Honda *et al.*, "Wavelength-shifted protection for WDM-PON with AMCC scheme for 5 G mobile fronthaul," in *Proc. Opt. Fiber Commun. Conf. Exhib.*, San Diego, CA, USA, Mar. 2019, pp. 1–3, Paper W3J.6.

[2] "40-Gigabit-cable passive optical networks (NG-PON2): General requirements," ITU-T Recommendation G.989.1, Mar. 2013.

[3] S. Shibita, D. Hisano, K. Mishina, and A. Maruta, "Demonstration of reflected interference cancellation in single-wavelength bidirectional PON system," in *Proc. IEEE Photon. Conf.*, San Antonio, TX, USA, 2019, pp. 1–2.
[4] K. Y. Cho, Y. J. Lee, H. Y. Choi, A. Murakami, A. Agata, and Y. Takushima, "Effects of reflection in RSOA-Based WDM PON utilizing remodulation technique," *J. Lightw. Technol.*, vol. 27, no. 10, pp. 1286–1295, May 2009.
[5] N. Cheng, L. Zhou, X. Liu, and F. J. Effenberger, "Reflective crosstalk cancellation in self-seeded WDM PON for mobile fronthaul/backhaul," *J. Lightw. Technol.*, vol. 34, no. 8, pp. 2056–2063, Apr. 2016.
[6] Z. V. Ruben *et al.*, "Self-homodyne detection-based fully coherent reflective PON using RSOA and simplified DSP," *Photon. Technol. Lett.*, vol. 27, no. 21, pp. 2226–2229, Nov. 2015.
[7] K. Kasai, Y. Wang, M. Yoshida, T. Hirooka, K. Iwatsuki, and M. Nakazawa, "80 gbit/s/ch, 256 QAM digital coherent optical transmission system with injection-locking for next generation mobile fronthaul network," in *Proc. Eur. Conf. Opt. Commun.*, 2017, pp. 1–3, Paper Th.1.B.5.
[8] J. Pan, C. Liu, T. Detwiler, A. J. Stark, Y. Hsueh, and S. E. Ralph, " Inter-channel crosstalk cancellation for Nyquist-WDM superchannel applications," *J. Lightw. Technol.*, vol. 30, no. 24, pp. 3993–3999, Dec. 2012.
[9] K. Shibahara, A. Masuda, S. Kawai, and M. Fukutoku, "Multi-stage successive interference cancellation for spectrally-efficient super-nyquist transmission," in *Proc. Eur. Conf. Opt. Commun.*, Valencia, 2015, pp. 1–3, 2015, Paper Th.1.6.4.
[10] M. Nakazawa, "Rayleigh backscattering theory for single-mode optical fibers," *J. Opt. Soc. Amer.*, vol. 73, no. 9, pp. 1175–1180, Sep. 1983.
[11] D. Hisano, S. Shibita, K. Mishina, Y. Nakayama, K. Maruta, and A. Maruta, "Wavelength swapping scheme to eliminate reflected light in bidirectional WDM-PON," in *Proc. OSA Adv. Photon. Congr.*, 2020, pp. 1–2, Paper JTu3F.3.